

Galileo AltBOC Receiver

Jean-Marie Sleewaegen, Wim De Wilde ([Septentrio NV, Belgium](#))
Martin Hollreiser ([ESA-ESTEC, The Netherlands](#))

ABSTRACT

Alternative BOC, AltBOC(15,10) modulation on E5, is one of the most advanced and promising signals the Galileo satellites will transmit. Galileo receivers capable of tracking this signal will benefit from unequalled performance in terms of measurement accuracy and multipath suppression.

However, the signal processing techniques required to process the AltBOC modulation are much more challenging than those for the traditional BPSK or even for the usual BOC modulation. This stems from the extremely large bandwidth and from the complex interaction of 4 components of the spreading code. Despite a high number of publications on the tracking of other Galileo signals, little has been published yet on the tracking of AltBOC.

The purpose of this paper is to present the principles of tracking and receiver-side processing for the AltBOC(15,10) signal. First, the signal structure is discussed in detail. Then the principle of demodulation and the architecture of the tracking channel are discussed alongside with related algorithms. The hardware implementation of the prototype receiver is presented as well. Finally, the impact of various error sources on the tracking performance is evaluated.

INTRODUCTION

Galileo is to transmit four different signals in the E5 band. Two of them will carry navigation messages whilst two are data-free pilot channels.

Signal component	Modulation	Data	Center frequency
E5aI	BPSK(10)	Yes	1176.45MHz
E5aQ	BPSK(10)	No	
E5bI	BPSK(10)	Yes	1207.14MHz
E5bQ	BPSK(10)	No	

Table 1 Main characteristics of the four components of the E5 signal band.

In this paper, it is assumed that the four signal components in the E5 band are modulated as a single wideband signal generated following the AltBOC(15,10) 8-PSK modulation as described and

analysed in [1, 2, 3]. This wideband signal is centered at the E5 frequency of 1191.795MHz, and has a bandwidth of at least 70 MHz.

The AltBOC modulation offers the advantage that the E5a (I&Q) and E5b (I&Q) bands can be processed independently, as traditional BPSK(10) signals, or together, leading to tremendous performances in terms of tracking noise and multipath.

Unlike most previous publications, this paper focuses on the AltBOC signal from a receiver perspective. After a brief description of the AltBOC modulation and demodulation principle, the noise and multipath errors are evaluated on both the code and carrier measurements, and the influence of the receiver frontend bandwidth is assessed. Also, the signal distortion due to the ionosphere dispersion within the E5 band is analysed.

AltBOC SIGNAL STRUCTURE

For the derivation of the demodulation principle of the AltBOC modulation, it is sufficient to approximate the baseband AltBOC signal by its AltLOC counterpart:

$$s(t) = d_1(t)c_1(t)e^{j\omega_s t} + d_2(t)c_2(t)e^{-j\omega_s t} + c_3(t)e^{j(\omega_s t + \pi/2)} + c_4(t)e^{-j(\omega_s t - \pi/2)}$$

where

- $c_1(t)$ is the PRN code of the E5b-data component (E5bI) and $d_1(t)$ is the corresponding bit modulation;
- $c_2(t)$ is the PRN code of the E5a-data component (E5aI) and $d_2(t)$ is the corresponding bit modulation;
- $c_3(t)$ is the PRN code of the E5b-pilot component (E5bQ);
- $c_4(t)$ is the PRN code of the E5a-pilot component (E5aQ);
- the exponential factors represent the sub-carrier modulation of E5a and E5b;
- ω_s is the side-band offset pulsation: $\omega_s = 2\pi f_s$, with $f_s = 15.345\text{MHz}$.

In reality, to meet the requirement for a constant envelope, $s(t)$ contains additional product terms and the sub-carrier exponentials are quantized. This effect has been taken into account in all the performance plots in this paper, but will not be explicitly included in the equations for the sake of clarity. $s(t)$ is modulated on the E5 carrier at 1191.795MHz.

AltBOC DEMODULATION AND TRACKING

The analysis is performed for the pilot channel, formed by the combination of E5aQ and E5bQ. The data channel case will be addressed shortly at the end of this section.

The AltBOC pilot signal is composed of the c_3 and c_4 components:

$$s_P(t) = c_3(t)e^{j(\omega_s t + \pi/2)} + c_4(t)e^{-j(\omega_s t - \pi/2)}$$

In principle each component could be demodulated by correlating $s_P(t)$ with the c_r -sequence multiplied by the complex conjugate of the corresponding sub-carrier exponential, e.g. to track the $c_3(t)$ component, the receiver must correlate with $c_3(t)e^{-j(\omega_s t + \pi/2)}$.

The corresponding correlation function ($C_{E5bQ}(\tau)$) can easily be derived (assuming an infinite signal bandwidth):

$$C_{E5bQ}(\tau) = \int_{T_{\text{int}}} c_3(t) e^{j(\omega_s t + \frac{\pi}{2})} c_3(t - \tau) e^{-j(\omega_s (t - \tau) + \frac{\pi}{2})} dt$$

$$\propto \text{triangle}(\tau) e^{j\omega_s \tau}$$

where:

- $\text{triangle}(\tau) = \begin{cases} 1 - |\tau| & |\tau| < T_c \\ 0 & \text{otherwise} \end{cases}$;
- τ is the delay between the incoming signal and the local code and sub-carrier replicas;
- T_{int} is the integration time;
- T_c is the chip length in units of time.

$C_{E5bQ}(\tau)$ is represented in Figure 1. It can be seen that it is a complex function of τ . If the local code and sub-carrier replicas are misaligned, energy moves from the I- to the Q-branch. Such a correlation peak cannot be tracked as the code and carrier misalignments are not clearly separated: any code misalignment leads to a carrier phase tracking error.

As the carrier loop is generally much faster than the code loop, it will tend to zero the energy in the Q branch, resulting in the code loop seeing a pure BPSK correlation peak.

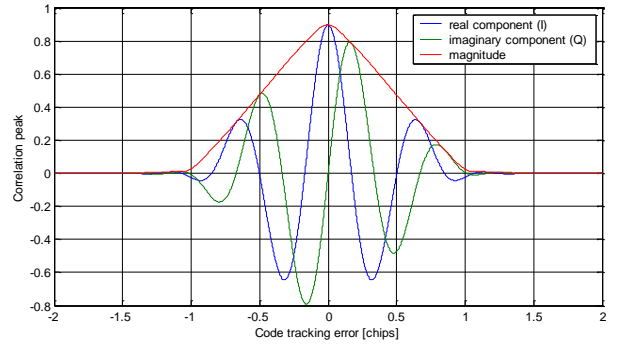


Figure 1 Single-component complex correlation peak.

The additional information needed to make use of the BOC principle is the fact that the other side-band is coherently transmitted at a frequency distance of exactly $2f_s = \omega_s/\pi$.

The $C_{E5aQ}(\tau)$ correlation function is given by correlating $s_P(t)$ with $c_4(t)e^{j(\omega_s t - \pi/2)}$:

$$C_{E5aQ}(\tau) = \int_{T_{\text{int}}} c_4(t) e^{-j(\omega_s t - \frac{\pi}{2})} c_4(t - \tau) e^{j(\omega_s (t - \tau) - \frac{\pi}{2})} dt$$

$$\propto \text{triangle}(\tau) e^{-j\omega_s \tau}$$

A Fresnel diagram as plotted in Figure 2 provides an intuitive view of the complex $C_{E5aQ}(\tau)$ and $C_{E5bQ}(\tau)$ correlations.

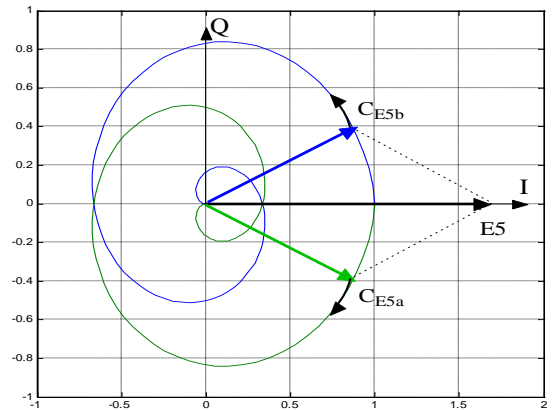


Figure 2 C_{E5aQ} and C_{E5bQ} correlation vectors in a Fresnel diagram.

In this diagram, both correlations are represented as vectors in the I,Q plane. As the code delay τ increases, C_{E5bQ} and C_{E5aQ} rotate with an angle $+\omega_s \tau$ and $-\omega_s \tau$ respectively, and their amplitude decreases

according to the triangle function, leading to the two helixes as shown in the figure.

A combined correlation peak can be derived by summing the C_{E5aQ} and C_{E5bQ} correlations, which corresponds to summing the vectors in Figure 2:

$$C_{E5Q}(\tau) = C_{E5bQ}(\tau) + C_{E5aQ}(\tau) = \text{triangle}(\tau) \cdot \cos(\omega_s \cdot \tau)$$

$C_{E5Q}(\tau)$ is real for all code delays, and hence can be used for code tracking. It is the AltBOC correlation peak, as represented in Figure 3.

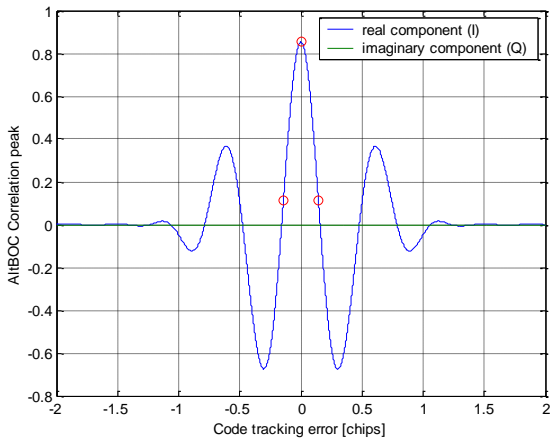


Figure 3 AltBOC correlation peak (70MHz bandwidth), and possible position of the E, P and L correlators, assuming an early-late spacing of 0.3 chips (red circles).

As can be seen in Figure 4, the AltBOC(15,10) correlation peak is similar in shape to the BOC(15,10), but its main peak is steeper, leading to better tracking performances.

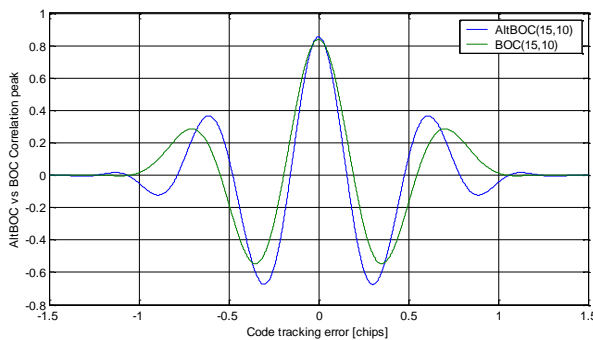


Figure 4 Comparison of the AltBOC(15,10) and BOC(15,10) correlation peaks, assuming a signal bandwidth of 70MHz.

For the pilot channel, the combined E5a/E5b correlation is simply the sum of the individual E5a and E5b correlations. For the data channel, the same principle can be used, but the data bits have to be wiped off prior to the combination: the E5-data correlation peak is given by:

$$C_{E5I}(\tau) = d_1 C_{E5bI}(\tau) + d_2 C_{E5aI}(\tau) = \text{triangle}(\tau) \cdot \cos(\omega_s \cdot \tau)$$

This bit estimation process makes the tracking of the data channel less robust, especially at low C/N₀ where the probability of bit error is high.

RECEIVER MODEL

Processing the wideband AltBOC signal is challenging for the receiver for two main reasons:

- To process the AltBOC signal, the whole E5 band has to be downconverted through the same RF/IF chain. The minimal signal bandwidth is 50MHz (containing the main lobes only). This leads to sampling rates and clocking frequencies much higher than currently used in GPS receivers.
- The baseband signal processing is difficult due to the complex nature of the AltBOC baseband signal.

For the sake of the performance analysis performed in this paper, a simple demodulator model as presented in Figure 5 will be used.

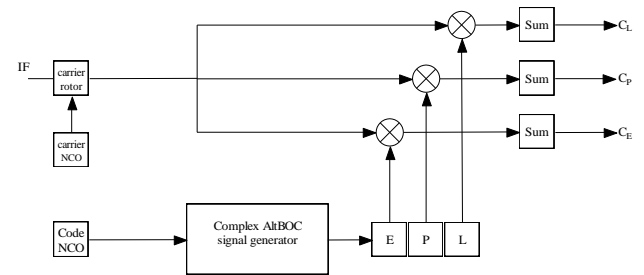


Figure 5 AltBOC channel architecture. All lines carry complex signals

Although the structure is the same as for a traditional BPSK receiver, the main difference is that all the operators (delay line, multiplications and sums) are complex.

The complex AltBOC signal generator produces a quantized version of the complex conjugate of the AltLOC baseband signal:

$$c_3(t) e^{-j(\omega_s t + \pi/2)} + c_4(t) e^{j(\omega_s t - \pi/2)}$$

The coherence between E5a and E5b allows to use the same code NCO for both bands.

CODE TRACKING NOISE

It is well known that the wideband AltBOC(15,10) signal will provide unprecedented code tracking performances.

Assuming that the code loop discriminator is of the dot-product power type and that the code is tracked using only the pilot channel, a general expression for the code tracking noise standard deviation for BPSK and BOC/AltBOC modulations is (expressed in meters):

$$\sigma_{code} = cT_c \sqrt{B_L \frac{1-R(d)}{2\alpha^2 \frac{C}{N_0}} \left(1 + \frac{1}{\frac{C}{N_0} T_p} \right)}$$

where

- d is the early-late spacing in chips
- $R(d)$ is the correlation peak evaluated at a delay of d , taking into account the signal filtering. For instance, for an unfiltered BPSK signal, $R(d)=1-d$.
- $\alpha = \left. \frac{dR(\tau)}{d\tau} \right|_{\tau=-\frac{d}{2}}$ is the slope of the correlation peak, evaluated at $\tau=-d/2$. For an unfiltered BPSK signal, $\alpha=1$, for an unfiltered BOC(n,m) signal, $\alpha=4n/m-1$, and for the AltBOC(15,10) signal in 70MHz with $d=0.3$, $\alpha=9$.
- B_L is the DLL loop bandwidth in Hz.
- T_p is the predetection integration time.
- C/N_0 is the carrier-to-noise ratio of the signal under consideration.
- c is the speed of light.
- T_c is the chip duration.

Figure 6 represents the code tracking noise as a function of the C/N_0 for different (non-PRS) modulation types used in Galileo and GPS. It is clear that the AltBOC largely outperforms the other codes, with a noise below 5cm down to a C/N_0 of 35dB-Hz. This is true even if only the pilot channel is tracked.

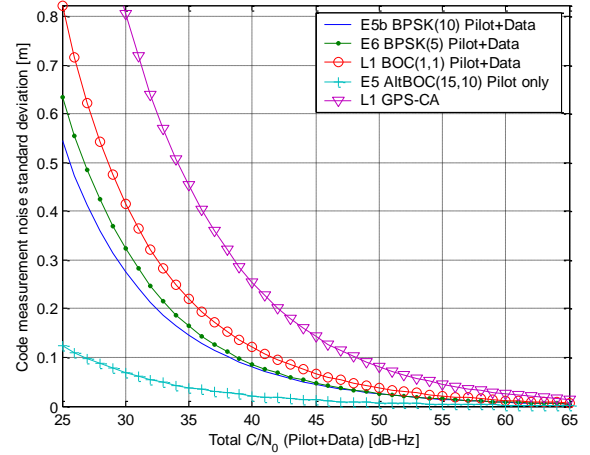


Figure 6 Code tracking noise of different codes planned for Galileo, and of GPS-CA.

CARRIER TRACKING NOISE

The AltBOC modulation does not directly improve the carrier tracking noise with respect to the BPSK modulation. Like for a BPSK signal, the carrier tracking noise standard deviation is given by (expressed in meters) [5]:

$$\sigma_{carrier} = \frac{\lambda_c}{2\pi} \sqrt{\frac{B_L}{C/N_0} \left(1 + \frac{1}{2T_p C/N_0} \right)}$$

where:

- B_L is the PLL loop bandwidth in Hz.
- T_p is the predetection integration time.
- C/N_0 is the carrier-to-noise ratio of the signal under consideration.
- λ_c is the carrier wavelength.

However, as the AltBOC signal is the coherent sum of the E5a and E5b components, the available C/N_0 will be 3dB higher than for a loop tracking E5a or E5b only. This will lead to a reduction by half of the noise variance.

CODE MULTIPATH ERROR

Besides the code tracking noise, code multipath performance is another argument in favour of the wideband AltBOC(15,10) modulation. As an example, the multipath error envelope for one multipath component with a signal-to-multipath ratio of 6dB is shown in Figure 7 for different modulations proposed for Galileo.

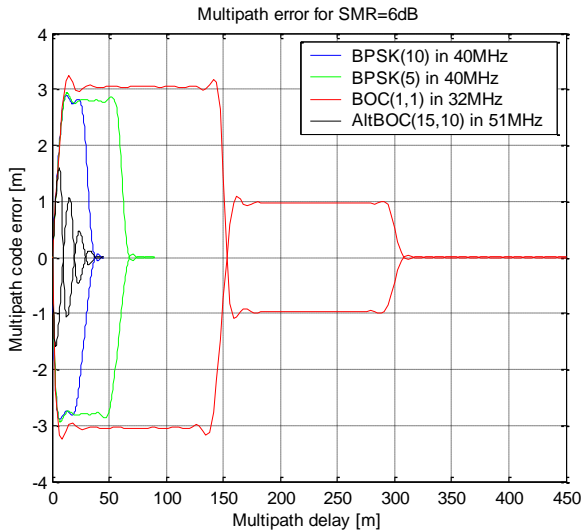


Figure 7 Comparison of the code multipath error envelopes for different modulations planned for Galileo, and for a signal-to-multipath power ratio of 6dB.

The inherent immunity to multipath of the AltBOC(15,10) modulation is clearly seen.

CARRIER MULTIPATH ERROR

Although less emphasis is put in the literature on the carrier phase multipath error, it is an important characteristic of a modulation when assessing the performance of precise carrier phase positioning.

In Figure 8, the carrier phase multipath error envelope of the AltBOC(15,10) modulation is compared to that of the BPSK(10) modulation (as present on E5a and E5b). The plot confirms the rule of thumb that the shape of the carrier multipath error envelope closely resembles the shape of the correlation peak.

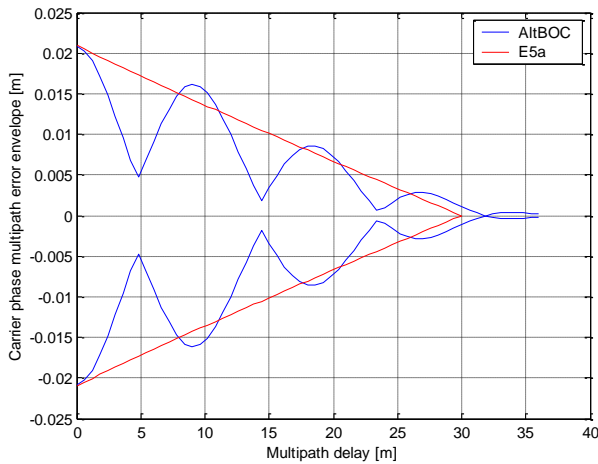


Figure 8 Carrier phase multipath envelope of the AltBOC and BPSK(10) modulation on E5, for a signal-to-multipath power ratio of 6dB.

It can be seen that the AltBOC modulation effectively decreases the multipath sensitivity of the PLL for some multipath delays. However, the improvement is not as dramatic as for the code multipath.

Comparing the code and carrier multipath error, as in Figure 9, it can be seen that the code error is zero when the phase error is maximum and vice versa. This is a general property of the BOC modulations, which applies to AltBOC as well.

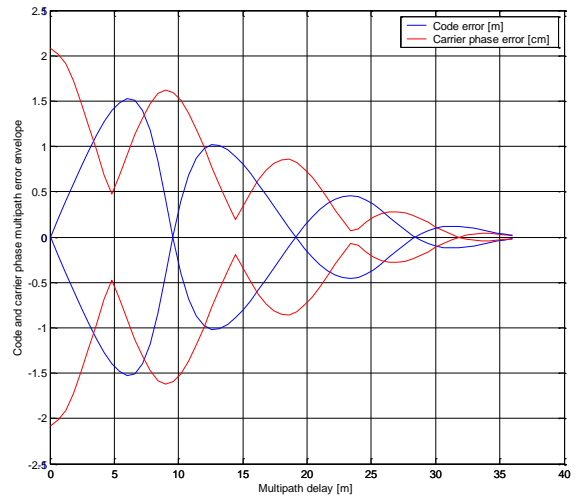


Figure 9 Comparison of the AltBOC code and carrier multipath error envelope.

INFLUENCE OF SIGNAL BANDWIDTH

A major challenge when designing an AltBOC receiver is to support the large bandwidth of the signal.

In this section, the effect of the signal bandwidth is analysed. Three different bandwidth are studied: 50 MHz (the main lobes only), 70 MHz and 90 MHz.

In the analysis, it is assumed that the sampling frequency (F_s) is equal to the double-sided signal bandwidth, and that the Early-Late spacing is given by $2 \cdot 10.23 \text{ MHz} / F_s$.

Correlation Peak

The correlation peak is plotted in Figure 10 for the three considered bandwidths, and for the infinite bandwidth as reference.

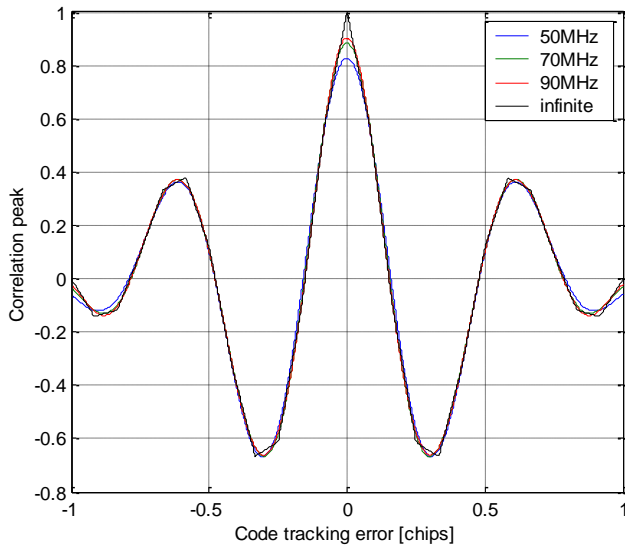


Figure 10 Comparison of the AltBOC correlation peak for different signal bandwidths.

It can be seen that the main effect of increasing the bandwidth is to increase the signal power, given by the value of the correlation at zero delay. Otherwise, the shape of the correlation is not significantly affected.

Code Noise

Figure 11 shows the code noise standard deviation for the three bandwidths under consideration. Compared to the 50-MHz case, the noise standard deviation is 15% smaller at 70 MHz, and 20% smaller at 90 MHz. This reduction stems partly from the increase in power, and partly from the reduction of the E-L spacing when higher bandwidths are used.

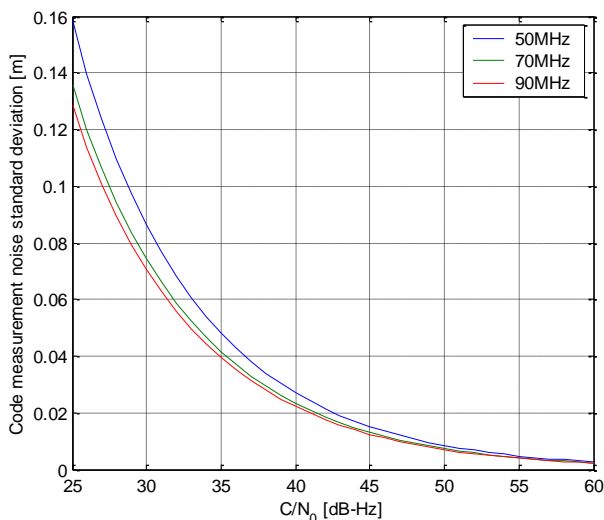


Figure 11 Comparison of the AltBOC code tracking noise for different signal bandwidths.

Code Multipath

Code multipath errors for the three bandwidths is plotted in Figure 12. It can be seen that increasing the bandwidth does not lead to a significant reduction of the multipath error.

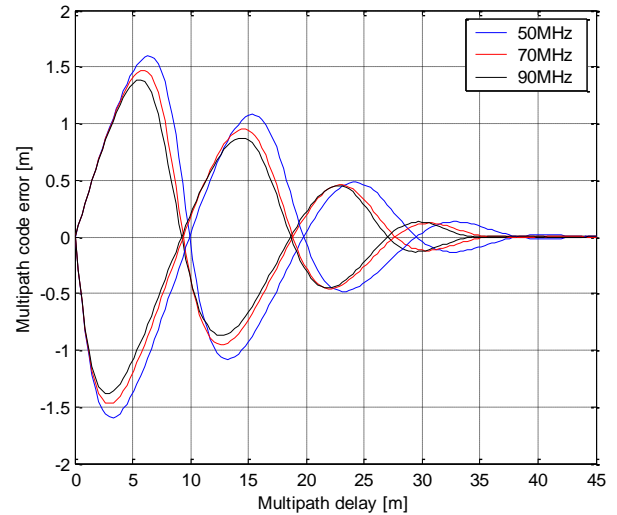


Figure 12 Comparison of the AltBOC code multipath error for different signal bandwidths.

Carrier Noise and Carrier Multipath

The carrier noise and multipath are not significantly affected by the signal bandwidth (apart from the fact that there is slightly more signal power when not filtering the side lobes, leading to a slight decrease of the noise).

EFFECT OF THE IONOSPHERIC DISPERSION

In GPS, it is well known that the ionosphere causes the L1 modulation to arrive in advance with respect to the L2 modulation. However, dispersion within the L1 and L2 bands is considered negligible. Due to the large bandwidth of the AltBOC signal, this assumption might not be correct for Galileo in case of high ionosphere activity, leading to potential signal distortion.

The effect of the ionosphere dispersion within the E5 band is analysed in this section. It will be shown that, even for large ionosphere activity, no significant distortion is expected.

We will start by assuming that the advance of the E5 carrier due to the passage through the ionosphere is t_0 (in units of time). It is well-known [4] that the time advance of any other carrier at a frequency f can be accurately approximated by:

$$\tau_{\varphi}(f) = I_0 \left(\frac{f_{E5}}{f} \right)^2$$

This time advance can be expressed as a phase shift (in cycles):

$$\varphi(f) = f\tau_{\varphi}(f) = I_0 \left(\frac{f_{E5}}{f} \right)^2 f = I_0 \frac{f_{E5}^2}{f}$$

Note that the time advance of the modulation (i.e. the opposite of the group delay) is given by:

$$\tau_c(f) = \frac{\partial \varphi(f)}{\partial f} = -I_0 \left(\frac{f_{E5}}{f} \right)^2$$

and it can be seen that $\tau_{\varphi}(f) = -\tau_c(f)$, which is the well-known fact that the code delay is opposite to the phase advance.

To analyse the distortion caused by the ionosphere, we need to remove from $\varphi(f)$ the phase shift that would be induced by a non-dispersive ionosphere.

If the ionosphere was not dispersive around E5, the code delay would be I_0 ($\tau_{c,0}(f) = -I_0$) over the whole E5 band, and the phase shift would be (expressed in cycles):

$$\begin{aligned} \varphi_0(f) &= \int \tau_{c,0}(f) df \\ &= -\int I_0 df \\ &= -I_0 f + 2I_0 f_{E5} \end{aligned}$$

where the integration constant is determined by the constraint that $\varphi_0(f_{E5}) = I_0 f_{E5}$. As can be seen in Figure 13, $\varphi_0(f)$ is simply the tangent to $\varphi(f)$ at the E5 frequency.

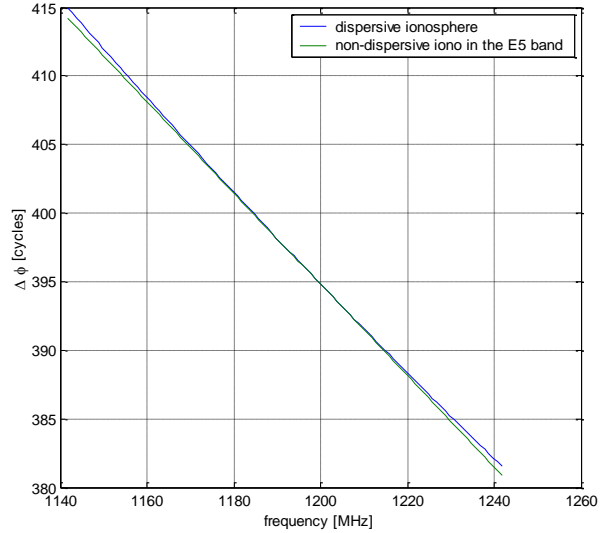


Figure 13 Phase shift introduced by the ionosphere ($\varphi(f)$), and the same phase shift if the ionosphere was not dispersive in the E5 band ($\varphi_0(f)$).

The signal distortion induced by the ionosphere can be modelled by applying a phase shift of $\varphi(f) - \varphi_0(f)$ to the signal. This phase shift is represented in Figure 14.

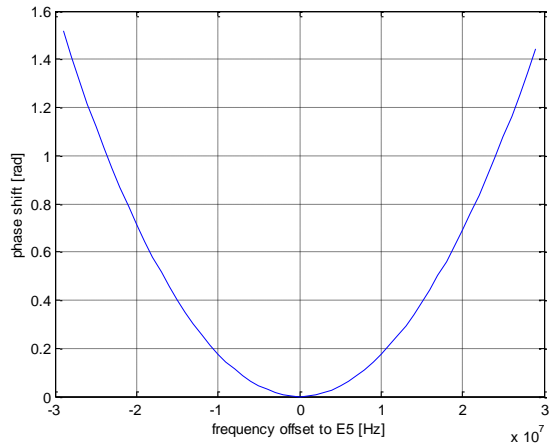


Figure 14 Phase shift introduced by the ionosphere (excluding the non-dispersive terms).

Namely, if $X(f)$ is the Fourier transform of the AltBOC signal before entering the ionosphere, the Fourier transform of the distorted signal after passing through the ionosphere is given by:

$$Y(f) = X(f) \cdot e^{j2\pi(\varphi(f) - \varphi_0(f))}$$

and the distorted signal is the inverse Fourier transform of $Y(f)$.

The correlation peak of such a distorted signal has been computed for the case of $I_0 = 0.33\mu\text{s}$ at E5,

which corresponds to 100m if expressed in units of length, which can be considered as a worst case condition. The result is plotted in the lower panel of Figure 15.

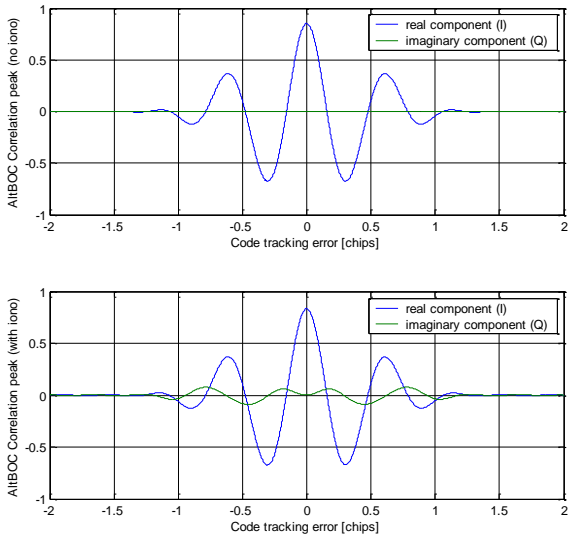


Figure 15 AltBOC correlation peak without ionosphere dispersion (above), and with (below), assuming an ionosphere delay of 100m on E5.

It can be seen that the signal distortion causes the correlation to leak through the imaginary component. The PLL forces the imaginary component to be zero at a delay of zero, which can be seen in Figure 15.

The ionosphere dispersion does not cause a significant loss of signal power: the amplitude of the correlation is only 2% smaller, even with the selected worse ionosphere condition.

Due to the peak distortion, the PLL and DLL will exhibit some tracking error. However, it seems that these errors are very small: they remain lower than a few centimetres for both the PLL and DLL, even for the worst-case ionosphere considered here.

For instance, the component of the carrier phase error caused by the ionosphere dispersion within the E5 band (excluding the constant and first order terms) is plotted in Figure 16, as a function of the ionosphere delay on E5.

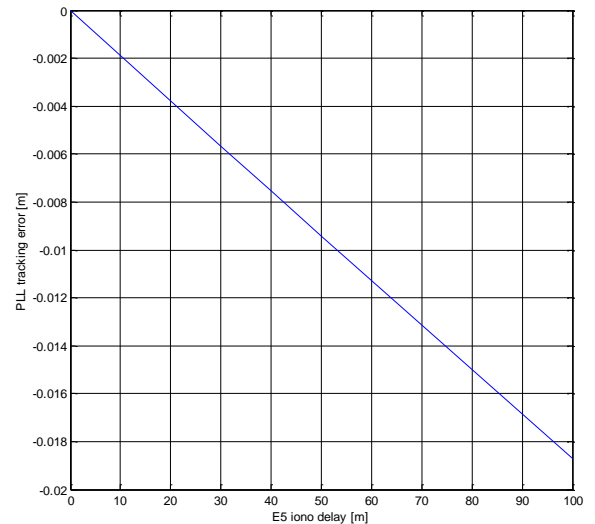


Figure 16 E5 PLL bias caused by the ionosphere dispersion within the E5 band as a function of the ionosphere delay.

It is likely that this bias will be negligible in most practical situations. In RTK positioning for instance, it will affect both the base station and the rover, such that it will cancel out in the difference.

CONCLUSIONS

This paper presented the AltBOC modulation from a receiver perspective. It has been shown that the major challenge in supporting the AltBOC signal is its large bandwidth and the complex nature of the baseband signal.

Although the AltBOC modulation primarily benefits the code noise and code multipath, it has been demonstrated that the carrier multipath performance is improved as well.

It has been shown that processing the full bandwidth of the AltBOC signal does not significantly improve the performance with respect to processing the main lobes only.

Finally, the impact of the ionosphere dispersion within the E5 band has been evaluated, and it has been shown that the effect, though not zero, will be insignificant for most practical applications.

ACKNOWLEDGMENT

The authors are thankful to ESA for their financial and programmatic support. Most parts of this work have been performed under ESA-ESTEC Contract 17932/03/NL/DS

REFERENCES

[1] *A Software Simulation Tool for GNSS2 BOC Signals*, L Ries et al, ION GPS 2002, September 2002.

[2] *New Investigations on Wideband GNSS2 Signals*, L Ries et al, GNSS 2003, April 2003.

[3] *Comparison of AWGN Code Tracking Accuracy for Alternative-BOC, Complex-LOC and Complex-BOC Modulation Options in Galileo E5-Band*, M. Soellner and Ph. Erhard, GNSS 2003, April 2003.

[4] *GPS Signal Structure and Performance Characteristics*, Navigation, Journal of the ION, Vol. 25, No.2, pp 121-146, Summer 1978.

[5] *Satellite Signal Acquisition and Tracking*, P. Ward, in "Understanding GPS Principle and Applications", edited by E.D. Kaplan, Artech House, 1996.